J|A|C|S
ARTICLES
Published on Web 02/02/2008

# Assessment of Chemically Separated Carbon Nanotubes for Nanoelectronics

Li Zhang,[†] Sasa Zaric,[†] Xiaomin Tu,[‡] Xinran Wang,[†] Wei Zhao,[‡] and Hongjie Dai*,[†]

*Department of Chemistry and Laboratory for Advanced Materials, Stanford University, Stanford, California 94305 and Department of Chemistry, University of Arkansas, Little Rock, Arkansas 72204*

Received November 28, 2007; E-mail: hdai@stanford.edu; wxzhao@ualr.edu

***Abstract:*** It remains an elusive goal to obtain high performance single-walled carbon-nanotube (SWNT) electronics such as field effect transistors (FETs) composed of single- or few-chirality SWNTs, due to broad distributions in as-grown materials. Much progress has been made by various separation approaches to obtain materials enriched in metal or semiconducting nanotubes or even in single chiralties. However, research in validating SWNT separations by electrical transport measurements and building functional electronic devices has been scarce. Here, we performed length, diameter, and chirality separation of DNA functionalized HiPco SWNTs by chromatography methods, and we characterized the chiralities by photoluminescence excitation spectroscopy, optical absorption spectroscopy, and electrical transport measurements. The use of these combined methods provided deeper insight to the degree of separation than either technique alone. Separation of SWNTs by chirality and diameter occurred at varying degrees that decreased with increasing tube diameter. This calls for new separation methods capable of metallicity or chirality separation of large diameter SWNTs (in the ~1.5 nm range) needed for high performance nanoelectronics. With most of the separated fractions enriched in semiconducting SWNTs, nanotubes placed in parallel in short-channel (~200 nm) electrical devices fail to produce FETs with high on/off switching, indicating incomplete elimination of metallic species. In rare cases with a certain separated SWNT fraction, we were able to fabricate FET devices composed of small-diameter, chemically separated SWNTs in parallel, with high on-/off-current ($I_{on}/I_{off}$) ratios up to $10^5$ owing to semiconducting SWNTs with only a few ($n$,$m$) chiralities in the fraction. This was the first time that chemically separated SWNTs were used for short channel, all-semiconducting SWNT electronics dominant by just a few ($n$,$m$)'s. Nevertheless, the results suggest that much improved chemical separation methods are needed to produce nanotube electronics at a large scale.

## Introduction

Single-walled carbon nanotubes have attracted much attention for possible applications in molecular electronics,[1−3] optoelectronics,[4−6] drug delivery,[7,8] and chemical and biological sensors.[9,10] An important and long-standing goal of SWNTs has been large-scale purely semiconducting SWNTs for high performance electronics such as FETs, aimed at potentially replacing silicon devices in future circuits. To maximize the performance of nanotube FETs, it is desirable to obtain SWNTs with similar diameter, chiralities and thus band-gaps, and connect them in parallel to build each FET device for sufficient on-currents and reproducible device characteristics. The lengths of SWNTs should also be controllable to meet the requirement of desired channel length. One of the most significant obstacles to the application of SWNTs in nanoelectronics has been separation according to their length, diameter, and chirality.

Much progress was made by various separation and metal vs semiconductor selection approaches, including electrical breakdown,[11] dielectrophoresis,[12] density differentiation,[13] size-exclusion chromatography (SEC),[14] ion-exchange chromatography (IEC),[15−17] and selective chemical functionalization or etching of nanotubes.[18,19] Separation of SWNTs by IEC obtained

[†] Stanford University.
[‡] University of Arkansas at Little Rock.

(1) Bachtold, A.; Hadley, P.; Nakanishi, T.; Dekker, C. *Science* **2001**, *294*, 1317−1320.
(2) Wind, S. J.; Appenzeller, J.; Martel, R.; Derycke, V.; Avouris, P. *Appl. Phys. Lett.* **2002**, *81*, 1359.
(3) Javey, A.; Guo, J.; Wang, Q.; Lundstrom, M.; Dai, H. *Nature* **2003**, *424*, 654−657.
(4) Arnold, M. S.; Sharping, J. E.; Stupp, S. I.; Kumar, P.; Hersam, M. C. *Nano Lett.* **2003**, *3*, 1549−1554.
(5) Freitag, M.; Martin, Y.; Misewich, J. A.; Martel, R.; Avouris, P. *Nano Lett.* **2003**, *3*, 1067−1071.
(6) O'Connell, M. J.; Bachilo, S. M.; Huffman, C. B.; Moore, V. C.; Strano, M. S.; Haroz, E. H.; Rialon, K. L.; Boul, P. J.; Noon, W. H.; Kittrell, C.; Ma, J. P.; Hauge, R. H.; Weisman, R. B.; Smalley, R. E. *Science* **2002**, *297*, 593−596.
(7) Bianco, A.; Prato, M. *Adv. Mater.* **2003**, *15* (20), 1765−1768.
(8) Kam, N. W. S.; Dai, H. *J. Am. Chem. Soc.* **2005**, *127*, 6021−6026.
(9) Chen, R. J.; Bangsaruntip, S.; Drouvalakis, K. A.; Kam, N. W. S.; Shim, M.; Li, Y. M.; Kim, W.; Utz, P. J.; Dai, H. J. *Proc. Natl. Acad. Sci. U.S.A.* **2003**, *100*, 4984−4989.
(10) Star, A.; Joshi, V.; Han, T. R.; Altoe, M. V. P.; Gruner, G.; Stoddart, J. F. *Org. Lett.* **2004**, *6*, 2089−2092.
(11) Collins, P. C.; Arnold, M. S.; Avouris, P. *Science* **2001**, *292*, 706−709.
(12) Krupke, R.; Hennrich, F.; Lohneysen, H.; Kappes, M. M. *Science* **2003**, *301* (5631), 344−347.
(13) Arnold, M. S.; Green, A. A.; Hulvat, J. F.; Stupp, S. I.; Hersam, M. C. *Nat. Nanotechnol.* **2006**, *1*, 60−65.
(14) Huang, X.; Mclean, R. S.; Zheng, M. *Anal. Chem.* **2005**, *77*, 6225−6228.


**10.1021/ja7106492 CCC: $40.75** 

a semiconducting to metallic SWNT ratio of ~9:1.[15,16] CoMoCAT SWNTs (in the diameter range of $d \approx 0.7-1.1$ nm) separated by chirality and laser-ablation grown SWNTs (in diameter range of $d \approx 1.1-1.6$ nm) separated by metallicity were reported by the density differentiation method.[13] Recently, the combination of SEC and IEC yielded chirality separated CoMoCAT SWNTs.[17] The degree of SWNT separation was typically characterized by atomic force microscopy (AFM), optical absorption, Raman spectroscopy, and photoluminescence spectroscopy. Despite achieving SWNT electronics as a major aim of chemical separation, research in validating SWNT separations by electrical transport measurements and advanced electronic devices has been scarce. SWNTs separated by the SEC and IEC method have not been made into electrical devices for characterization of SWNTs or device performance analysis. Long-channel (~20 $\mu$m) devices formed by short, density-gradient separated and percolating SWNT networks have been made with on-/off-current ($I_{on}/I_{off}$) switching ratios up to $\sim 10^4$.[13] However, high $I_{on}/I_{off}$ short-channel FETs formed by multiple semiconducting SWNTs fully spanning the channel length have not been demonstrated for separation methods thus far. This would be an important goal of SWNT transistors while providing an ultimate validation to the completeness of chemical separation of semiconducting vs metallic SWNTs.

Here, with the aim of obtaining SWNTs for potentially high performance electronics, we carried out separation of DNA-functionalized HiPco single-walled carbon nanotubes (SWNTs) by length using size-exclusion chromatography SEC, and subsequent diameter, metallicity, and chirality separation by ion-exchange chromatography IEC. Photoluminescence excitation/emission (PLE) spectroscopy was used for the first time to characterize the (*n*,*m*) chiralities of SWNTs in SEC/ IEC separations and evaluate the degree of separation. We found that the IEC method was effective in separating semiconducting SWNTs by chirality and diameter at varying degrees that decrease with increasing SWNT diameter. Further, we fabricated nanoelectronic devices comprising length- and diameter-separated SWNTs in parallel, and obtained field effect transistors (FETs) with high $I_{on}/I_{off}$ ratios, owing to semiconducting SWNTs enriched in only a few (*n*,*m*) chiralities. Electrical transport provided further analysis of the remaining metallic nanotubes in semiconductor dominant fractions.

## Methods

SWNTs used in this study are the as-grown HiPco nanotubes purchased from Carbon Nanotechnologies Incorporated (CNI). Single-stranded DNA (ssDNA) sequence, $d(GT)_{20}$ from Integrated DNA Technologies, Inc., was used for CNT dispersion. All other chemicals were purchased from Sigma-Aldrich, unless otherwise specified.

**Dispersion and Separation of SWNTs.** SWNT dispersion by ssDNA, SEC separation, and IEC separation were conducted according to the procedures described previously,[14−16] with some changes outlined below. As grown HiPco tubes were ultrasonically dispersed with $d(GT)_{20}$ solution. For length separation, after centrifugation to remove bundled and non-soluble materials, the entire dispersion solution was fractionated by three SEC analytical columns with pore sizes of 2000, 1000, and 300 Å (Sepax Technologies, Inc.) in series in a Waters Breeze HPLC system with the elution collected at 0.25 mL/fraction and labeled by the collection sequences (SEC1 through SEC30). The length-separated fractions of more than 10 runs were collected and concentrated with optical density >1 (path length = 1 mm) for the IEC step. A volume of 600 $\mu$L of SEC-purified carbon nanotubes with narrow length distribution was injected into an anion-exchange column NS 1500 (75 mm by 7.8 mm, Biochrom Labs, Inc.) in the Waters Breeze HPLC system, which was then eluted in a linear salt gradient (0−0.9 M NaSCN in 20 mM MES buffer at pH 7.0) with a 40-mL volume at a flow rate of 2.0 mL/min. Starting from 4 min of the elution time, fractions were collected every 15 s, and the fractions were labeled again as the collection sequences (IEC1 through IEC40). By using a centrifugal filter (Millipore, 30000 MWCO), the fractions were exchanged with $D_2O$ several times to remove the salts for optical measurement and device fabrication.

**Absorption Spectra Measurements.** The samples in $D_2O$ were hosted in 1-mm path-length quartz cells, and their absorption spectra were measured in the 350−1500 nm range using a Varian Cary 5000 UV−vis−NIR spectrophotometer. $D_2O$ was used as a reference for background subtraction.

**Photoluminescence Excitation/Emission Spectroscopy.** Photoluminescence excitation/emission (PLE) measurements were performed utilizing a home-built setup. A short arc lamp (Osram XBO 75W/2 OFR 75 W xenon lamp installed into Oriel 66907 Arc Lamp Source) and a monochromator (Oriel 7400 Cornerstone 130 monochromator) were used to supply the excitation light in the 550−840 nm range in 10-nm steps. The excitation light was focused onto a sample placed in a 1-mm path quartz cuvette. The room-temperature sample photoluminescence was collected at the opposite cuvette wall, and the PL spectrum was recorded using a second monochromator (Acton SpectraPro 2300i) and a liquid nitrogen-cooled InGaAs array detector (Princeton Instruments OMA V 1024−2.2 LN) in the 900−1450 nm range. The obtained PL spectra were scaled according to the measured excitation power (measured using Oriel 71580 calibrated Si photodiode) before obtaining PLE spectrum by interpolating the measured 30 PL spectra. The bandpass used for emission and excitation was 15 nm.

**Atomic Force Microscopy.** SWNTs in the separated fractions of sample solution was deposited onto a piece of Si substrate pretreated with 3-aminopropyltriethoxysilane (APTES, 12 mL in 20 mL $H_2O$) to enhance the adsorption of DNA-functionalized nanotubes, and rinsed with water and dried. The sample was then calcined in air at 300 °C for 10 min to remove the DNA. Tapping mode AFM (Digital Instruments multimode) was used to acquire images of SWNTs on the substrate under ambient conditions.

**Electrical Device Fabrication and Characterization.** Deposition of SWNTs from separated fractions on substrates for device fabrication was the same as above except that the substrate used was Si with thermally grown $SiO_2$ (100-nm thick with 10-nm thick regions). The substrates were heated in 1.4 Torr $H_2$ to 800 °C for 10 min to anneal the nanotubes. The SWNTs were randomly distributed on the substrate with high density, and we placed arrays of metal source/drain (S/D) electrode pairs (S/D width of ~10 $\mu$m, channel length of ~200−300 nm) to contact multiple SWNTs (average number of ~ 15) between each S/D pair. Electron-beam lithography was used to define the S/D regions. The probing pads were in the 100-nm $SiO_2$ region of the substrate and channel region was in the 10 nm $SiO_2$ regions. Pd (20 nm) was used as the S/D metal. The samples were annealed at 220 °C in an Ar atmosphere for better contacts between the metal and the tubes. A Hewlett-Packard 4156B semiconductor analyzer was used to measure the electrical properties of the devices.

(15) Zheng, M.; Jagota, A.; Semke, E. D.; Diner, B. A.; Mclean, R. S.; Lustig, S. R.; Richardson, R. E.; Tassi, N. G. *Nat. Mater.* **2003**, *2*, 338−342.
(16) Zheng, M.; Jagota, A.; Strano, M. S.; Santos, A. P.; Barone, P.; Chou, S. G.; Diner, B. A.; Dresselhaus, M. S.; Mclean, R. S.; Onoa, G. B.; Samsonidze, G. G.; Semke, E. D.; Usrey, M.; Walls, D. J. *Science* **2003**, *302*, 1545−1548.
(17) Zheng, M.; Semke, E. D. *J. Am. Chem. Soc.* **2007**, *129*, 6084−6085.
(18) Strano, M. S.; Dyke, C. A.; Usrey, M. L.; Barone, P. W.; Allen, M. J.; Shan, H.; Kittrell, C.; Hauge, R. H.; Tour, J. M.; Smalley, R. E. *Science* **2003**, *301*, 1519−1522.
(19) Zhang, G.; Qi, P.; Wang, X.; Lu, Y.; Li, X.; Tu, R.; Bangsaruntip, S.; Mann, D.; Zhang, L.; Dai, H. *Science* **2006**, *314*, 974−977.

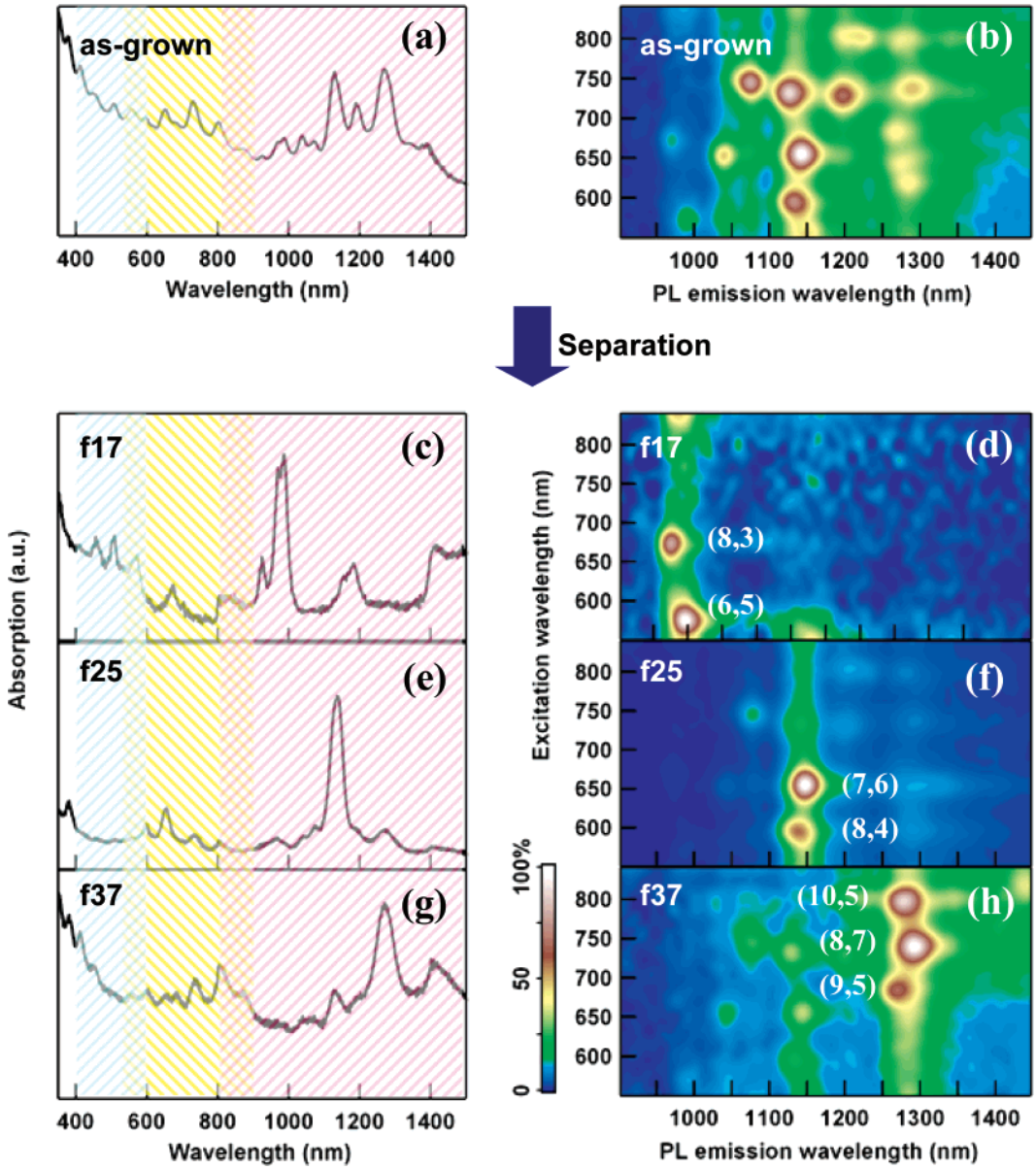


***Figure 1.*** Chemically separated carbon nanotubes characterized by optical absorption and photoluminescence spectroscopy. Parts a and b are spectra for the starting HiPco SWNTs functionalized by DNA. Parts c−h are data for SWNT fractions after SEC−IEC separations. Parts c and d are for fraction f17. Parts e and f are for fraction f25. Parts g and h are for fraction f37. In the absorption spectra, the wavelength ranges of lowest energy semiconducting, second lowest semiconducting, and lowest metallic absorption peaks are shaded red, yellow, and blue, respectively.

## Results and Discussion

**Spectroscopic Characterizations of Separated SWNTs.** It is well-known that as-grown HiPco SWNTs contain a mixture of metallic and semiconducting nanotubes with wide (*n*,*m*) chirality distribution, as can be seen from UV−vis−NIR and PLE spectra of the as-grown SWNT/DNA solution (Figure 1, parts a and b). The HiPco SWNTs have various semiconducting tubes showing first sub-band $E_{11}$ UV−vis−NIR absorption peaks in the 800−1600 nm range and second subband $E_{22}$ absorption peaks in the 550−900 nm range (Figure 1a).[20] The distribution of (*n*,*m*) of semiconducting SWNTs can also be seen from PLE data (Figure 1b). Metallic SWNTs are not reflected from PLE spectra of the samples, but can be gleaned from UV−vis−NIR absorption spectrum since they exhibit absorption peaks in the 400−600 nm region (Figure 1a) due to $E_{11}$ transitions between sharp van Hove singularities of metallic-bands.[21]

The SEC and IEC separated fractions of SWNTs showed much simpler and fewer peak structures in UV−vis−NIR and PLE spectra in the first and the second subband range than the starting HiPco sample (Figure 1, parts c, e, g, d, f, and h). From PLE data (Figure 1, parts d, f, and h), the most prominent chiralities of semiconducting SWNTs in the separated samples were (8,3) and (6,5) in the fraction SEC24-IEC17 (named f17 here-on), (7,6) and (8,4) in the fraction SEC24-IEC25 (f25), and (10,5), (8,7), and (9,5) in the fraction SEC25-IEC37 (f37). The SWNT diameters are $d \approx 0.78$ and 0.76 nm in f17, $d \approx 0.90$ and 0.84 nm in f25, and $d \approx 1.05$, 1.03, and 0.98 nm in

(20) Bachilo, S. M.; Strano, M. S.; Kittrell, C.; Hauge, R. H.; Smalley, R. E.; Weisman, R. B. *Science* **2002**, *298*, 2361−2366.

(21) O'Connell, M. J.; Bachilo, S. M.; Huffman, C. B.; Moore, V. C.; Strano, M. S.; Haroz, E. H.; Rialon, K. L.; Boul, P. J.; Noon, W. H.; Kittrell, C. *Science* **2002**, *297*, 593−596.

f37, respectively, indicating diameter separation between IEC fractions. We observed that the number of chiralities in the separated fractions increased as the fraction's average diameter increased (Figure 1, parts d, f, and h), suggesting a decrease in separation efficiency for larger diameter SWNTs by the IEC method.

This was the first time that photoluminescence excitation/emission or PLE spectroscopy was used to analyze SWNTs separated by the SEC/IEC method. PLE provided useful information difficult to attain by UV−vis−NIR spectroscopy alone. UV−vis−NIR spectra of some of the separated fractions showed an apparent, single intense $E_{11}$ absorption peak, whereas PLE data clearly distinguished similar diameter SWNTs with different chiralities contributing to the same $E_{11}$ absorption peak (Figure 1, parts d, f, and h). The relative photoluminescence intensities could also be used to estimate the degree of enrichment of certain (*n*,*m*) SWNTs in a fraction relative to other fractions. For instance, in fraction f25, the ratio between photoluminescence intensities of $d \approx 0.9$ nm (7,6) and (8,4) SWNTs and $d \approx 1$ nm (10,5), (8,7) (9,5) SWNTs was ∼10 vs a ratio of ∼2.0 in the as-grown material, suggesting an enrichment factor of ∼5 for (7,6) and (8,4) SWNTs in f25 over the $d \approx 1$ nm tubes. Similar analysis found that in f37, the $d \approx 1$ nm SWNTs were enriched by a factor of ∼5.8 over the smaller $d \approx 0.9$ nm SWNTs.

UV−vis−NIR spectra provided information about metallic SWNTs not attained in PLE data, since the lowest energy absorption peaks of metallic SWNT show up in the 400−600 nm range. We found that the fraction f25 exhibited relatively fewer absorption peaks in this range than other fractions, e.g., f37 (Figure 1, part e vs part g), indicating fewer metallic SWNTs in the (8,4) and (7,6) dominant fraction f25 than in the larger diameter fraction f37. Nevertheless, quantification of the residue metallic species in these fractions based on spectroscopy data was not straightforward, for which we carried out electrical transport measurements as described below.

**Atomic Force Microcopy of Separated SWNTs.** We used AFM to further characterize the separated SWNTs. Since the SWNTs were length-separated by SEC prior to diameter/metallicity separation by IEC, we indeed observed that SWNTs in the fractions SEC24 and SEC25 were of high purity with uniform length distribution around 300 nm (Figure 2, parts a, b, and inset of c). In fact, we selected the SEC fractions 24 and 25 for further IEC separation, due to the relatively long SWNTs in these fractions useful for later device fabrication. Other SEC fractions, such as those with lengths down to ∼50−100 nm, were not used in the current work. AFM clearly revealed that the diameters of SWNTs in f25 were smaller than those in f37 (Figure 2c), with measured heights of 1.20 ± 0.11 nm in f25 and 1.37 ± 0.14 nm in f37. These results were larger than the diameters of (*n*,*m*) SWNTs based on absorption and PLE data, which could be due to the DNA coating on the tubes, as our calcination step may not have completely removed the coating. It is also possible that the AFM topography over-estimates the diameter of SWNTs due to van der Waals distances between SWNT/substrate and SWNT/AFM tip. Notably, the AFM data showed that the smaller-diameter fraction f25 exhibited a narrower diameter distribution than the larger-diameter f37 (Figure 2c), suggesting more effective diameter separation for the earlier IEC fractions in the smaller diameter region. This

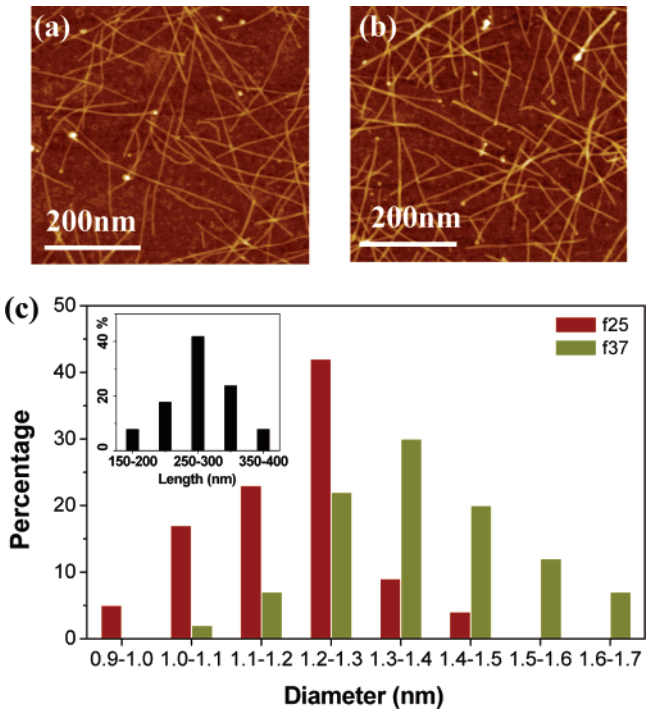


***Figure 2.*** Microscopy data on diameter and length separation of SWNTs. Parts a and b are AFM images of SWNTs in fractions f25 and f37, respectively. Part c is the histogram of the diameters of SWNTs in the two fractions, determined from topographic height measurements. The mean measured diameter of tubes in f25 is 1.20 ± 0.11 nm and 1.37 ± 0.14 nm in f37. Inset shows the length distribution of nanotubes in the fractions.

was also consistent with the results based on spectroscopy analysis (Figure 1).

**Electrical Properties of Separated SWNTs.** To characterize the electrical properties and investigate chemically separated SWNTs for nanoelectronics, we fabricated short-channel FET-like devices (Figure 3a, gate oxide thickness ≈ 10 nm) using the semiconductor-enriched SWNTs. The channel length of the devices was $L \approx 200-300$ nm. AFM imaging of the devices showed that the average connections of each device were $N \approx 15$ tubes (Figure 3, parts b and e). Most of the nanotubes were directly bridging the source (S) and drain (D) electrodes although a small fraction of tubes showed crossing and was connected to S/D through each other. The large number of SWNTs in each device presented a test to the degree of enrichment for semiconducting SWNTs, since a single metallic tube spanning the S/D could short the device electrically and prevent the device from switching off. Note that the crossing SWNTs relaxed the rigor of the test since a metallic tube connecting to a semiconducting SWNT could still give high on/off ratios. For f25 enriched in (8,4) and (7,6) SWNTs, we found from the histogram of $I_{on}/I_{off}$ ratios of the devices (Figure 4) that a substantial fraction (nearly 50%) of the devices exhibited high $I_{on}/I_{off}$ ratios ($>10^2$), indicating most of the SWNTs in this fraction were indeed semiconducting in nature, consistent with the UV−vis−NIR data (Figure 1e). In contrast, electrical devices of SWNTs from the larger diameter fraction f37 exhibited very low $I_{on}/I_{off}$ ratio, with only ∼5% of devices with $I_{on}/I_{off}$ of ∼10. This result suggested that out of $N \approx 15$ tubes in fraction f37 existed ≥1 metallic tubes.

The UV−vis−NIR absorption data (Figure 1) suggested the enrichment of semiconducting SWNTs relative to metallic ones,

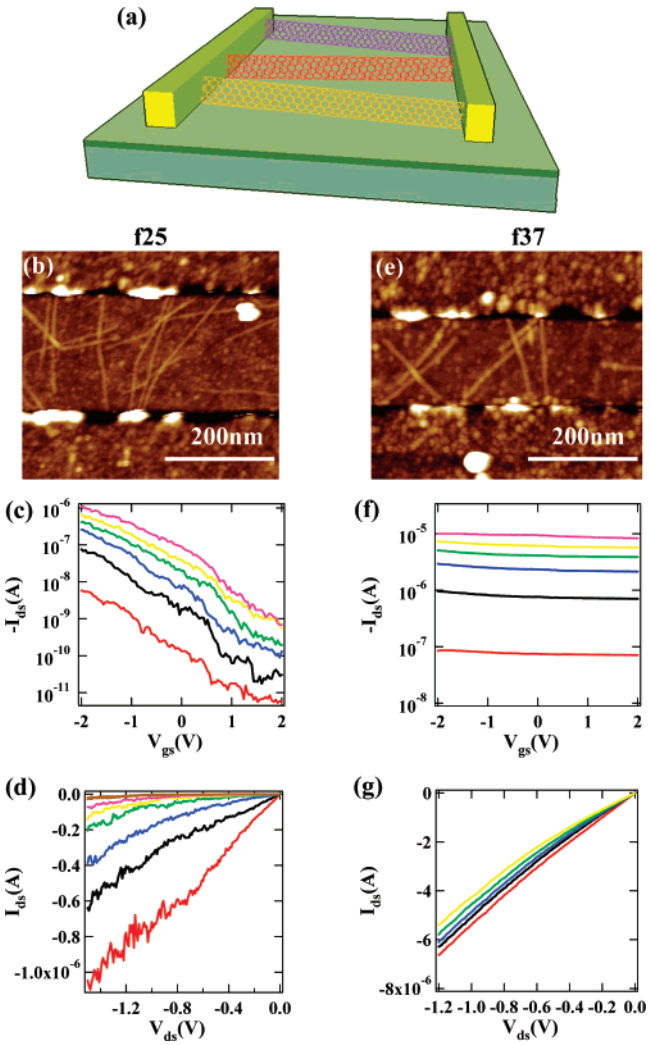


***Figure 3.*** Electrical transport measurements and devices of chemically separated SWNTs. (a) A schematic drawing of our device comprised of multiple chemically separated SWNTs ($N \approx 15$) bridging a pair of source-drain electrodes. (b) AFM image of the part of a typical device made from SWNTs in fraction f25. (c) Transfer characteristics ($I_{ds}-V_{gs}$ curves) of the device at different bias voltages $V_{ds}$ = 10, 100, 300, 500, 700, and 1000 mV from bottom to top. (d) Current−voltage characteristics ($I_{ds}-V_{ds}$) of the device at different $V_{gs}$ from −2 to 1 V with the step of 500 mV from bottom to top. Parts e, f, and g are AFM data, transfer characteristics $I_{ds}-V_{gs}$, and current−voltage $I_{ds}-V_{ds}$ characteristics of a typical device made from SWNTs in fraction f37. The $I_{ds}-V_{ds}$ curves correspond to various $V_{gs}$ from −2 to 2 V with the step of 1 V from bottom to top.

though the unknown and different absorption coefficient of different chirality SWNTs prevented us from estimating the ratio of semiconducting to metallic nanotubes in the separated fractions. We were able to glean this information from the electrical measurements on the devices made from the desired nanotube fractions (Figure 3 and 4). For devices made of SWNTs in fraction f25 enriched in (8,4) and (7,6) tubes, about 41% exhibited $I_{on}/I_{off} > 10^2$, indicating all nanotubes (average number $\approx$ 15) in each of these devices were semiconductors (Figure 4). This suggested that ~94% (i.e., $0.94^{15} \approx 41\%$) of the SWNTs in f25 were semiconductors, which are mainly (7,6) and (8,4) tubes according to the PLE spectrum (Figure 1f). In other words, semiconducting (7,6) and (8,4) SWNTs are highly enriched in fraction f25, leading to depletable FET devices composed of SWNTs with mostly the two chiralities. However, similar devices made of SWNTs from the larger diameter

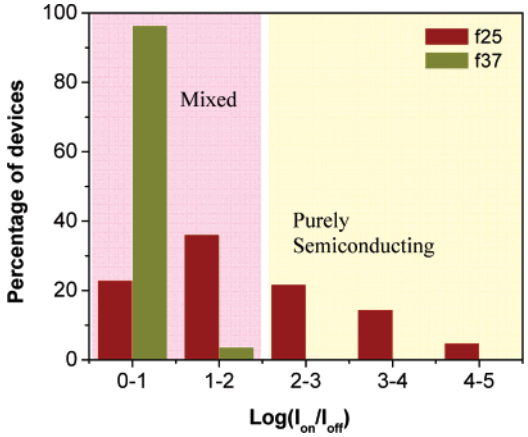


***Figure 4.*** Histograms of device percentages with various on-/off-current ($I_{on}/I_{off}$) ratios ($x$-axis) for devices made of SWNTs in fractions f25 and f37, respectively. Total number of devices measured for each fraction of tube is 98. Each device is composed of ~15 nanotubes bridging source/drain electrodes. High $I_{on}/I_{off}$ devices are composed of purely semiconducting SWNTs, whereas devices with low $I_{on}/I_{off}$ ratios are composed of mixture of metallic and semiconducting SWNTs due to incomplete separation.

fraction f37 afforded no purely semiconducting devices with sufficiently high $I_{on}/I_{off}$ ratios. Note that we used a relatively low $I_{on}/I_{off}$ ratio $>10^2$ as criterion for semiconducting SWNTs. This was because only very small diameter nanotubes are involved in the current work, and these tubes exhibited much lower on-current than larger diameter SWNTs in previous work[3,22] due to higher Schottky barriers and non-ohmic contacts.

It has been shown that IEC separates SWNTs according to their metallic or semiconducting nature.[15,16] The phosphate groups on the DNA provide negative charge on the surface of the carbon nanotube, which creates an electrostatic field along the tube axis and induces a positive screening image charge on metallic nanotubes. Therefore, metallic SWNTs have less surface negative charge and elute first, followed by the semiconducting SWNTs. The difference in the diameter of the semiconducting SWNTs produces variances in DNA wrapping geometry and the linear charge density.[16] Therefore, diameter-dependent separation of semiconducting SWNTs should take place simultaneously with the electronic separation. Our optical absorption data suggest that the amount of residue metallic SWNTs in the semiconductor-dominant fractions follows the trend of f25 < f37 < f17 (Figure 1), i.e., more residue metallic tubes exist in the smallest diameter fraction f17 enriched with the (6,5) tube (Figure 1c), followed by the larger diameter fraction f37 (Figure 1g). Metallic tubes in the intermediate fraction f25 appear to be the least (Figure 1e), consistent with the high $I_{on}/I_{off}$ ratios of the devices formed by SWNTs in f25 (Figures 3 and 4). The detailed mechanism underlying these observations is currently unknown and should be addressed in order to further improve the separation efficiency for electronics applications. For SEC, fractions are separated based on the size, i.e., the tube length (Figure 2, parts a, b, and the inset of c). Longer nanotubes are eluted earlier than shorter nanotubes. SEC and IEC are essentially independent to each other for length and metallicity separations respectively.

The performance of the multi-tube SWNT FETs based on f25 enriched in (8,4) and (7,6) SWNTs were excellent in high

(22) Kim, W.; Javey, A.; Tu, R.; Cao, J.; Wang, Q.; Dai, H. *Appl. Phys. Lett.* **2005**, *87*, 173101.

$I_{on}/I_{off}$ ratios up to $\sim 10^4$ (Figure 3c), superior to devices made of as-grown HiPco SWNT with a high metallic percentage. However, the on-current of $\sim 1$ $\mu$A for these devices (Figure 3d) was much lower than previously FETs made of SWNTs with larger diameters ($d > \sim 1.5$ nm) grown by chemical vapor deposition (CVD).[3] This was attributed to two factors, namely, poor contacts and lower carrier mobilities for smaller diameter SWNTs. Both Schottky barriers (SBs) and tunneling barriers exist between $d \approx 0.9-1.0$ nm SWNTs and the contact metal,[22] giving high contact resistance. Carrier mobility in smaller diameter semiconducting SWNTs may also be lower due to higher effective mass and shorter mean free path of scattering.[23] It is also likely that various defects exist in the separated SWNTs as a result of extensive sonication during dispersion and debundling. Nevertheless, the results of high $I_{on}/I_{off}$ short-channel SWNT FETs made of nanotubes with few chiralities (8,4) and (7,6) are encouraging. It validates chemical separation effects in enriching semiconducting nanotubes, and calls for future work to improve separation efficiency and device performance. Several approaches could enhance the performance of small diameter semiconducting SWNT transistors, including using heavy chemical doping of the metal-tube contacts to minimize SBs, and down-scaling the channel length to the 10−50 nm scale to minimize scattering and thus maximize the on current.[3] Alignment and packing of the separated SWNTs should also be devised, by developing deposition methods[14] or Langmuir−Blodgett (LB) approaches.[24] Chemical methods capable of metallicity and chirality separation of SWNTs with diameters in the 1.5 nm region are currently lacking and should be developed to obtain high performance nanotube electronics at a large scale.

(23) Zhou, X.; Park, J. Y.; Huang, S.; Liu, J.; McEuen, P. L. *Phys. Rev. Lett.* **2005**, *95*, 146805.

## Summary

In this work, we performed length, diameter, and chirality separation of DNA-functionalized HiPco SWNTs by chromatography methods, characterized the (*n,m*) chiralities of SWNTs by photoluminescence excitation spectroscopy, optical absorption spectroscopy, and electrical transport measurements. When combined, these methods provided deeper insight into the degree of separation than either technique alone. We fabricated FET devices composed of length, diameter, and chirality separated SWNTs in parallel, with high $I_{on}/I_{off}$ ratios up to $10^5$ owing to semiconducting (8,4) and (7,6) enriched SWNTs. This was the first time that chemically separated SWNTs are used for short channel, high $I_{on}/I_{off}$ switching SWNT transistors with just a few (*n,m*) tubes. Nevertheless, we find that separation of SWNTs by chirality and diameter occurred at varying degrees that decreases with increasing tube diameter. New separation methods capable of more complete separation,[25] and metallicity or chirality separation of large diameter SWNTs, are needed for future scalable, high-performance nanoelectronics.

**Acknowledgment.** This work was supported by MARCO-MSD and Intel.

JA7106492

(24) Li, X.; Zhang, L.; Wang, X.; Shimoyama, I.; Sun, X.; Seo, W. S.; Dai, H. *J. Am. Chem. Soc.* **2007**, *129*, 4890−4891.
(25) Li, X.; Tu, X.; Zaric, S.; Welsher, K.; Seo, W. S.; Zhao, W.; Dai, H. *J. Am. Chem. Soc.* **2007**, *129*, 15770−15771.